Chapter 6

Effect of Pre-Ratcheting on Tensile Properties of Alloys at RT

6.1 Introduction

This chapter discusses the effect of pre-ratcheting on tensile properties of modified 9Cr-1Mo steel and Inconel 617 alloy at room temperature. Similar studies were conducted by Rajpurohit et al., (2018) on Zircaloy-2 and by Dutta and Ray, (2013) on interstitial free steel. In the present investigation, fatigue tests were conducted on both the alloys mentioned above, varying different parameters such as mean stress, stress amplitude and stress rate for 200 asymmetrical stress cycles. The pre cyclically stressed specimens were tested under tensile loading, at a strain rate of 10^{-3} s^{-1}.

In the case of Inconel 617 alloy, the gap between the yield and ultimate tensile strength is very large; therefore, fatigue tests were conducted in two different regions i.e. (i) near the yield strength and (ii) near the ultimate tensile strength. The specimens failed under the tensile mode and the fractured ends of the tensile tested specimens were examined under scanning electron microscopy (SEM). Detailed microstructural characterization to observe the basic difference in deformation due to pre-ratcheting and to find the effect of the parameters was performed by transmission electron microscopy.

6.2 Effect of pre-ratcheting on tensile behaviour of the modified 9Cr-1Mo steel, at RT

In this section, the uniaxial ratcheting behaviour of modified 9Cr-1Mo steel under three different parameters (mean stress, stress amplitude and stress rate) has been discussed. Fatigue tests were conducted for 200 cycles; thereafter the same specimens were subjected to tensile loading, to observe the effect of pre-ratcheting, under the three different parameters, on tensile properties.

The percent change in the strength and ductility parameters, with respect to the un-ratcheted specimen, were calculated and fractographic analysis was carried out.

6.2.1 Tensile properties of the modified 9Cr-1Mo steel in normalized and tempered condition

The values of the 0.2 % offset yield strength (S_{YS}), ultimate tensile strength (S_{UTS}), uniform elongation (e_u), total elongation (e_f) and reduction in area (RA) are presented in Table 6.1 along with the values of the degree of strain hardening (S_{UTS}/ S_{YS}), strain hardening exponent (n), and strength coefficient (K).

Table 6.1 Tensile data of the modified 9Cr-1Mo steel at RT at 10^{-3} s^{-1}.

0.2% Yield Strength (MPa)	Ultimate Tensile Strength (MPa)	Elongation (%)	Uniform Plastic elongation (%)	Reduction in area (%)	Strength coefficient (K) (MPa)	Strain hardening exponent (n)	Degree of work hardening (S_{UTS} /S_{YS})
575	713	26	8	74	933	0.090	1.24

6.2.2 Uniaxial ratcheting behaviour of modified 9Cr-1Mo steel

Asymmetric stress cycling with tensile mean stress was carried out for 200 cycles, at RT, and was designated as pre-ratcheting. Asymmetric cyclic stressing with non- zero mean stress has been shown to generate hysteresis loops with opening, in Zircaloy-2 [Rajpurohit et al.,(2018)] and in steels [Dutta et al.,(2013)]. Fig. 6.1 shows the opening of the hysteresis loops and also the accumulation of ratcheting strain with cycles in the modified 9Cr -1 Mo steel.

The stress-strain loops may be seen to translate in the positive strain direction. There was maximum width and opening of the loop in the first cycle, and gradual reduction in the width as well as opening in the subsequent cycles. The test matrix for the pre-ratcheting is summarized in Table 6.2. Ratcheting fatigue testing was carried out for 200 cycles, at three different combinations of the test parameters.

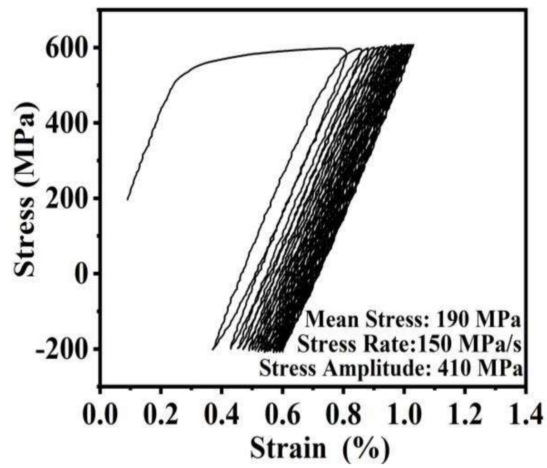

Fig. 6.1 Hysteresis loops of decreasing width resulting from ratcheting of modified 9Cr-1Mo steel.

Table 6.2 Test matrix for ratcheting fatigue tests of the modified 9Cr-1Mo steel, for 200 cycles, at RT.

Specimen No.	Maximum stress (σ_{max}) MPa	Minimum stress (σ_{min}) MPa	Mean stress (σ_m) MPa	Stress amplitude (σ_a) MPa	Stress rate ($\dot{\sigma}$) MPa/s
1	600	-220	**190***	**410***	**150***
2	610	-210	**200***	410	150
3	620	-200	**210***	410	150
4	600	-200	200	**400***	150
5	620	-220	200	**420***	150
6	610	-210	200	410	**50***
7	610	-210	200	410	**450***

******Variable*

Ratcheting behaviour of modified 9Cr-1Mo steel may be understood with the help of Fig. 6.2. The ratcheting strain increased with increase in the mean stress and stress amplitude, as shown in Fig. 6.2 (a and b). In contrast to the effects of mean stress and stress amplitude being increase in the ratcheting strain, there was decrement in the ratcheting strain with increase in the stress rate (Fig. 6.2c). As explained in the earlier Chapter 4, with increase in stress rate, the plastic strain energy as well as plastic strain per cycle decreased, due to higher cyclic work hardening of the material. This resulted from combined effects of higher number of dislocations produced at higher stress rate and less effective annihilation of dislocations, during the tensile and compressive load cycles. Thus, the overall density of dislocations was higher at higher stress rate, due to which the work hardening increases with increase in stress rate.

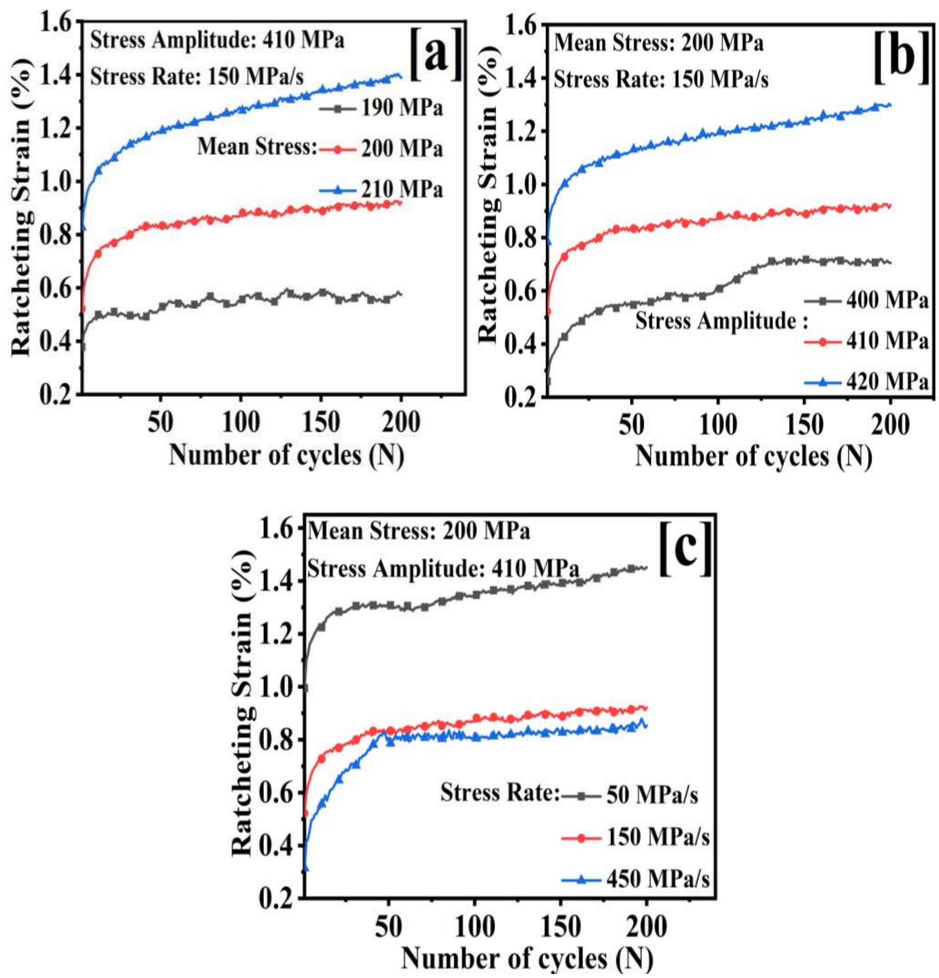

Fig. 6.2 Ratcheting behaviour of modified 9Cr-1Mo steel with different variables: (a) mean stress, (b) stress amplitude and (c) stress rate.

6.2.3 Tensile behaviour of the pre-ratcheted modified 9Cr-1Mo steel

The samples ratcheted for 200 cycles were subjected to tensile testing. Tensile parameters of the samples ratcheted for 200 cycles, for various combinations of test parameters, were examined with respect to that of the un-ratcheted sample.

(a) Tensile properties of the modified 9Cr-1Mo steel pre-ratcheted at various mean stresses

The tensile properties of the samples pre-ratcheted for 200 cycles, at variable mean stresses of 190, 200 and 210 MPa, at constant stress amplitude of 410 MPa and stress rate of 150 MPa/s, are summarized in Table 6.3. From the Table 6.3, it may be seen that strength parameters increased with respect to that of the un-ratcheted sample. With rise in the mean stress, there was enhancement of the yield strength, however, no definite trend was observed in variation of the ultimate tensile strength (Fig. 6.3a). The maximum increase in yield strength was about 20%. Uniform elongation as well as the degree of strain hardening decreased due to pre-ratcheting.

Table 6.3 Tensile data of modified 9Cr-1Mo steel pre-ratcheted at various mean stresses.

Mean stress σ_m (MPa)	Strength parameters			Ductility parameters			Work hardening parameters		Degree of work hardening
	Yield strength (MPa)	% Increase in Yield strength	Ultimate tensile strength (MPa)	Uniform Plastic elongation (%)	% Decrease in Uniform Plastic elongation	Total elongation (%)	Strength coefficient (MPa)	Strain hardening exponent	Ultimate tensile strength / Yield strength
Un-ratcheted	575	-	713	8.0	-	26.0	933	0.09	1.24
190	672	16.8	808	6.2	22.5	24.9	1126	0.10	1.20
200	678	17.9	792	6.1	23.7	24.2	1060	0.08	1.17
210	694	20.6	786	6.0	25.0	23.8	1080	0.09	1.13

(b) Tensile properties of the modified 9Cr-1Mo steel pre-ratcheted at various stress amplitudes

The tensile properties of the samples, pre-ratcheted to 200 cycles at varying stress amplitudes of 400, 410 and 420 MPa, at constant mean stress of 200 MPa and stress rate of 150 MPa/s, are summarized in Table 6.4. An effect, similar to that of the mean stress was observed. The strength parameters were increased considerably (Fig. 6.3b).

However, the degree of strain hardening and the uniform elongation were reduced after the pre- ratcheting.

Table 6.4 Tensile data of modified 9Cr-1Mo steel pre-ratcheted at various stress amplitudes.

Stress amplitude σ_a (MPa)	Strength parameters			Ductility parameters			Work hardening parameters		Degree of work hardening
	Yield strength (MPa)	% Increase in Yield strength	Ultimate tensile strength (MPa)	Uniform Plastic elongation (%)	% Decrease in Uniform Plastic elongation	Total elongation (%)	Strength coefficient (MPa)	Strain hardening exponent	Ultimate tensile strength / Yield strength
Un-ratcheted	575	-	713	8.0	-	26.0	933	0.09	1.24
400	663	15.3	804	6.9	13.7	25.7	1138	0.10	1.21
410	678	17.9	792	6.1	23.7	24.2	1060	0.08	1.17
420	686	19.3	799	5.6	30.0	22.7	1129	0.10	1.16

(c) Tensile properties of the modified 9Cr-1Mo steel pre-ratcheted at various stress rates

Table 6.5 Tensile data of modified 9Cr-1Mo steel pre-ratcheted at various stress rates.

Stress rate $\dot{\sigma}$ (MPa/s)	Strength parameters			Ductility parameters			Work hardening parameters		Degree of work hardening
	Yield strength (MPa)	% Increase in Yield strength	Ultimate tensile strength (MPa)	Uniform Plastic elongation (%)	% Decrease in Uniform Plastic elongation	Total elongation (%)	Strength coefficient (MPa)	Strain hardening exponent	Ultimate tensile strength / Yield strength
Un-ratcheted	575	-	713	8.0	-	26.0	933	0.09	1.24
50	689	19.8	763	6.8	15.0	24.4	989	0.07	1.11
150	678	17.9	792	6.1	23.7	24.2	1060	0.08	1.17
450	671	16.6	811	6.2	22.5	24.8	1121	0.09	1.20

The tensile properties of the specimens subjected to pre-ratcheting for 200 cycles; at variable stress rates of 50, 150 and 450 MPa/s, at constant mean stress of 200 MPa and stress amplitude of 410 MPa, are shown in Table 6.5. In contrast to increase in the yield strength with rise in the mean stress and stress amplitude, there is decrease in the yield strength with increase in the stress rate (Fig. 6.3c), due to fall in the strain hardening (Fig. 6.2c). The ultimate tensile strength followed a rising trend. The uniform elongation and the degree of work hardening decreased with respect to those of the un-ratcheted steel but did not follow a definite trend.

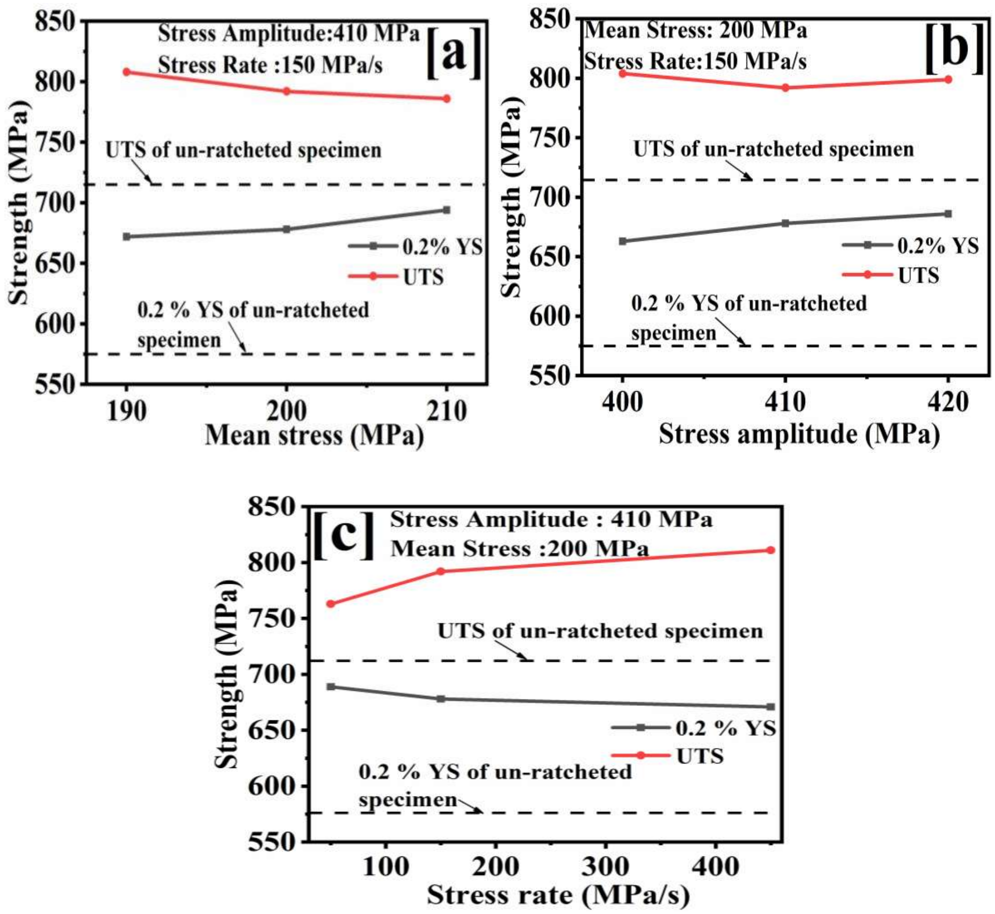

Fig. 6.3 Variation of 0.2% offset yield strength and ultimate tensile strength of modified 9Cr-1Mo steel, due to ratcheting variables: (a) mean stress, (b) stress amplitude and (c) stress rate.

6.2.4 Fracture Behaviour of modified 9Cr-1Mo steel

The fractographs of the un-ratcheted and ratcheted specimens are shown in Fig. 6.4 and 6.5 respectively. The un-ratcheted sample exhibited rosette fracture, with small fibrous central zone and large intermediate radial zones akin to rosette petals in the middle region, and a small shear lip zone at the outermost portion of the fracture surface (Fig. 6.4a). Fine dimples were seen in the central fibrous zone (Fig. 6.4b) in line with the earlier observation [Verma et al., (2017)].

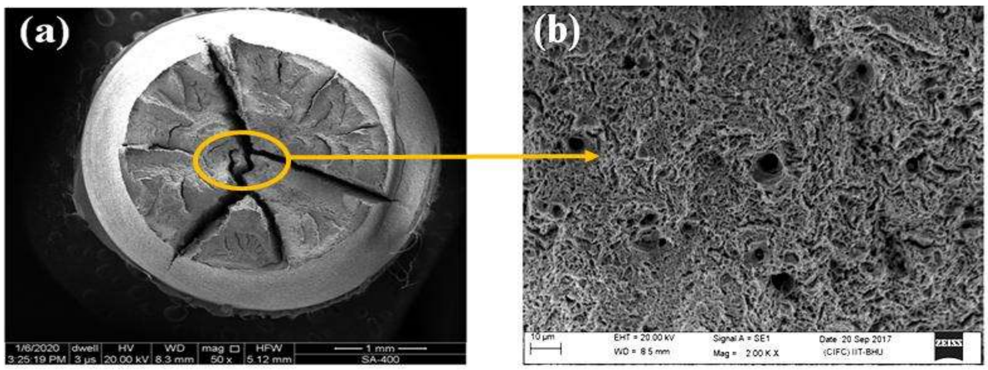

Fig. 6.4 Fractographs of the un-ratcheted tensile tested specimen of modified 9Cr-1Mo steel

On the other hand, the fractographs of the pre-ratcheted sample exhibited, both tensile and fatigue signatures (Fig. 6.5a). Fractured specimen revealed two distinct regions, an annular region and central region. While the central region showed dimples (Fig. 6.5b), the annular region revealed distinct features like fatigue striations (Fig. 6.5c). It is important to mention that these specimens were pre-ratcheted only for 200 cycles and were tested under tensile loading. Therefore, the observed ductile fracture with characteristic dimples is as expected and fatigue striations are not expected to be seen on the fracture surface. However, the circular region of the fractured specimens, close to fracture end shows striations like features because of progressive increase in length of the specimen, with number of cycles during pre-ratcheting.

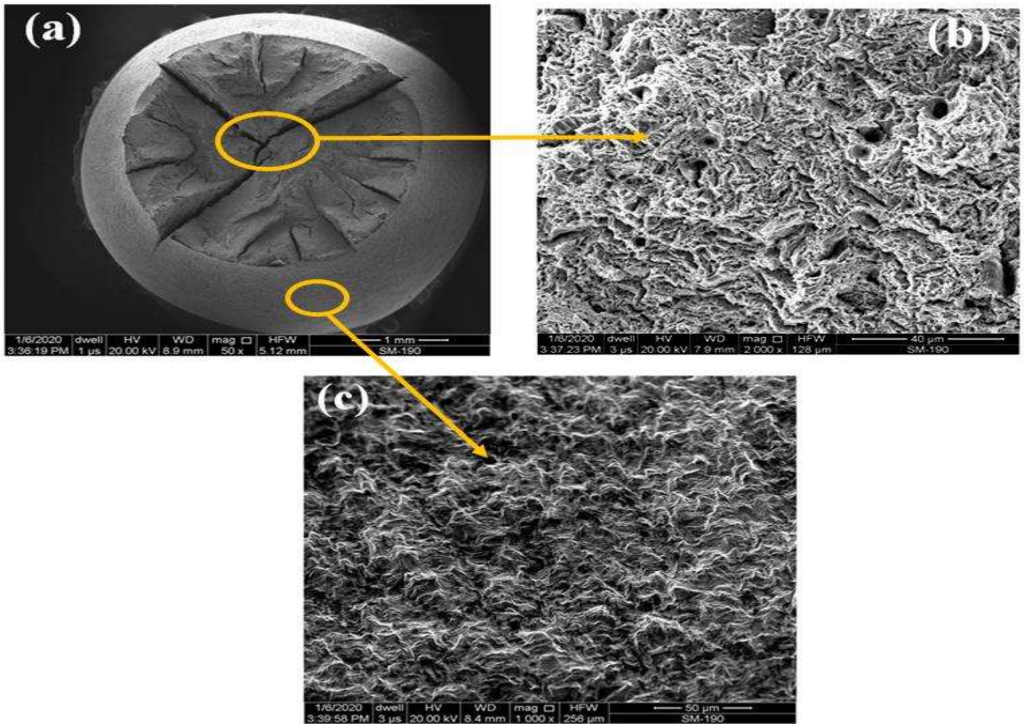

Fig. 6.5 Fracture behaviour of modified 9Cr-1Mo steel pre-ratcheted at mean stress of 190 MPa; stress amplitude of 410 MPa; and stress rate of 150 MPa/s and tensile tested: (a) at 200X, (b) enlarged view of the central region showing dimples and (c) enlarged view of the peripheral region showing striations like marks.

6.3 Effect of pre-ratcheting on tensile behaviour of Inconel 617 alloy at RT

In this section, the uniaxial ratcheting behaviour of Inconel 617 alloy at three different parameters (mean stress, stress amplitude and stress rate) has been discussed. The fatigue tests were conducted for 200 cycles and thereafter the same specimens were tested under tensile loading to examine the effect of pre-ratcheting on tensile properties. The effect of pre-ratcheting with the three parameters, on tensile properties, was studied. The percentage differences in the strength and ductility parameters with respect to the un-ratcheted specimen were calculated; also fractographic analysis was done of the tested samples.

6.3.1 Tensile properties of the Inconel 617 alloy in solution treated condition

The values of the 0.2 % offset yield strength (S_{YS}), ultimate tensile strength (S_{UTS}), uniform elongation (e_u), total elongation (e_f) and reduction in area (RA) are presented in Table 6.6 along with the values of the degree of strain hardening (S_{UTS}/ S_{YS}), strain hardening exponent (n), and strength coefficient (K).

Table 6.6 Tensile properties of the Inconel 617 alloy tested at strain rate of 10^{-3} s^{-1}, at RT.

0.2% Yield Strength (MPa)	Ultimate Tensile Strength (MPa)	Elongation (%)	Uniform Plastic elongation (%)	Reduction in area (%)	Strength coefficient (K) (MPa)	Strain hardening exponent (n)	Degree of work hardening (S_{UTS} /S_{YS})
347	835	66	54	68	1578	0.36	2.41

6.3.2 Uniaxial ratcheting behaviour of Inconel 617 alloy

Fig. 6.6 shows the hysteresis loops and accumulation of ratcheting strain, with number of cycles, resulting from the asymmetric cyclic stressing. The maximum width and opening of the loops were observed in the first cycle, and these were reduced in the subsequent cycles. Due to the tensile mean stress, acting on the specimen, the cyclic stress-strain loops were translated in the positive direction of strain.

The tensile properties mentioned in Table 6.6 clearly show that there is large gap between the yield strength and ultimate tensile strength of about 488 MPa. Therefore, to analyse the effect of pre-ratcheting on tensile properties, ratcheting fatigue tests were carried out for 200 cycles in two different regions, with the maximum stress close to the yield strength and with maximum stress near the ultimate tensile strength. The test matrix for pre-ratcheting in the above two regions is summarized in Tables 6.7 and 6.8.

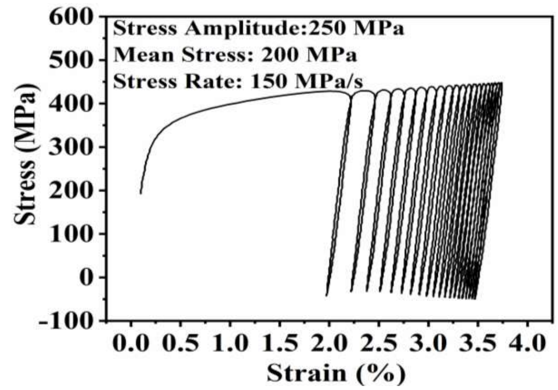

Fig. 6.6 Hysteresis loops resulting from ratcheting of Inconel 617 alloy.

Table 6.7 Test matrix for ratcheting fatigue tests up to 200 cycles for Inconel 617 alloy at RT, at maximum stress near the yield strength (S_{YS}).

Specimen No.	Maximum stress (σ_{max}) MPa	Minimum stress (σ_{min}) MPa	Mean stress (σ_m) MPa	Stress amplitude (σ_a) MPa	Stress rate ($\dot{\sigma}$) MPa/s
1	425	-75	**175***	**250***	**150***
2	450	-50	**200***	250	150
3	475	-25	**225***	250	150
4	425	-25	200	**225***	150
5	475	-75	200	**275***	150
6	450	-50	200	250	**50***
7	450	-50	200	250	**450***

******Variable*

Table 6.8 Test matrix for ratcheting fatigue tests up to 200 cycles for Inconel 617 alloy at RT, at maximum stress near the ultimate tensile strength (S_{UTS}).

Specimen No.	Maximum stress (σ_{max}) MPa	Minimum stress (σ_{min}) MPa	Mean stress (σ_m) MPa	Stress amplitude (σ_a) MPa	Stress rate ($\dot{\sigma}$) MPa
1	650	-350	**150***	**500***	**150***
2	700	-300	**200***	500	150
3	750	-250	**250***	500	150
4	650	-250	200	**450***	150
5	750	-350	200	**550***	150
6	700	-300	200	500	**50***
7	700	-300	200	500	**450***

******Variable*

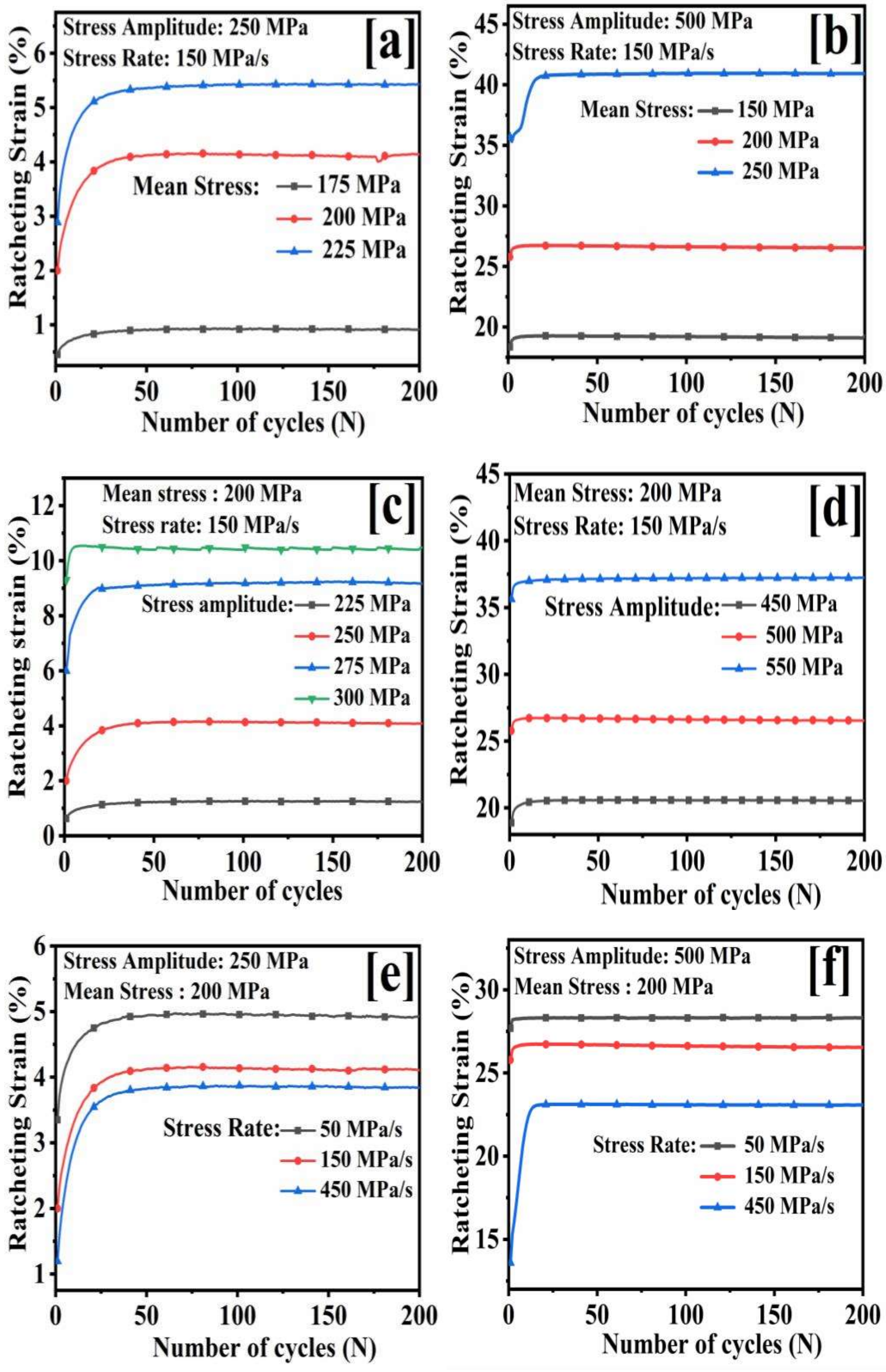

Fig. 6.7 Ratcheting fatigue behaviour of Inconel 617 alloy with various parameters: (a and b) mean stress (c and d) stress amplitude and (e and f) stress rate; at the maximum stress close to the yield strength and ultimate tensile strength.

Ratcheting behaviour of this alloy in two different regions may be easily understood with the help of Fig. 6.7. Ratcheting strain increases with increase in mean stress and stress amplitude as shown in Fig. 6.7(a, b, c and d). In contrast to this, ratcheting strain decreases with increase in stress rate as observed in Fig. 6.7(e and f).

6.3.3 Tensile behaviour of the Inconel 617 alloy pre-ratcheted with different parameters

The samples of Inconel 617 alloy ratcheted for 200 cycles with different parameters, in the regions close to the yield strength and the ultimate tensile strength, were subjected to tensile loading, at a strain rate of 10^{-3} s^{-1}, and tensile properties are compared with that of the un-ratcheted sample.

(a) Tensile properties of the Inconel 617 alloy pre-ratcheted at various mean stresses

Tensile behaviour of the Inconel 617 alloy, pre-ratcheted for 200 cycles near the yield strength, at variable mean stresses of 175, 200 and 225 MPa, at constant stress amplitude of 250 MPa and stress rate of 150 MPa/s are summarized in Table 6.9. Similarly, tensile properties of the pre-ratcheted alloy near the ultimate tensile strength, at different mean stresses of 150, 200 and 250 MPa, at constant stress amplitude of 500 MPa and stress rate of 150 MPa/s are summarized in Table 6.10. From the Tables 6.9 and 6.10, it is very clear that there is continuous increase in yield strength of the material with rise in the mean stress.

While the samples ratcheted near yield strength exhibited 44% increase, those ratcheted near the ultimate tensile strength exhibited marked increase of about 184% in the S_{YS}. Ultimate tensile strength of the ratcheted samples also increased as compared to that of the un-ratcheted one as depicted in Fig. 6.8 (a and b). Ductility parameters as well as the degree of work hardening decreased due to pre-ratcheting.

Table 6.9 Tensile data of the Inconel 617 alloy pre-ratcheted at different mean stresses, at maximum stress near the yield strength (S_{YS}).

Mean stress σ_m (MPa	Strength Parameters			Ductility Parameters			Work hardening Parameters		Degree of work hardening
	Yield strength (MPa)	% Increase in Yield strength	Ultimate tensile strength (MPa)	Uniform Plastic elongation (%)	% Decrease in Uniform Plastic elongation	Total elongation (%)	Strength coefficient (MPa)	Strain hardening exponent	Ultimate tensile strength / Yield strength
Un-ratcheted	347	-	835	54.5	-	66.6	1579	0.36	2.41
175	433	24.8	918	52.6	3.5	61.7	1750	0.36	2.12
200	474	36.6	859	51.0	6.4	61.0	1788	0.41	1.81
225	501	44.4	875	40.6	25.5	49.7	1704	0.35	1.74

Table 6.10 Tensile data of the Inconel 617 alloy pre-ratcheted at different mean stresses, at maximum stress near the ultimate tensile strength (S_{UTS}).

Mean stress σ_m (MPa	Strength Parameters			Ductility Parameters			Work hardening Parameters		Degree of work hardening
	Yield strength (MPa)	% Increase in Yield strength	Ultimate tensile strength (MPa)	Uniform Plastic elongation (%)	% Decrease in Uniform Plastic elongation	Total elongation (%)	Strength coefficient (MPa)	Strain hardening exponent	Ultimate tensile strength / Yield strength
Un-ratcheted	347	-	835	54.5	-	66.6	1579	0.36	2.41
150	713	105.5	888	37.2	31.7	48.9	1464	0.21	1.25
200	840	142.1	975	33.2	39.1	46.8	1557	0.18	1.16
250	987	184.4	1050	17.0	68.8	26.9	1450	0.10	1.06

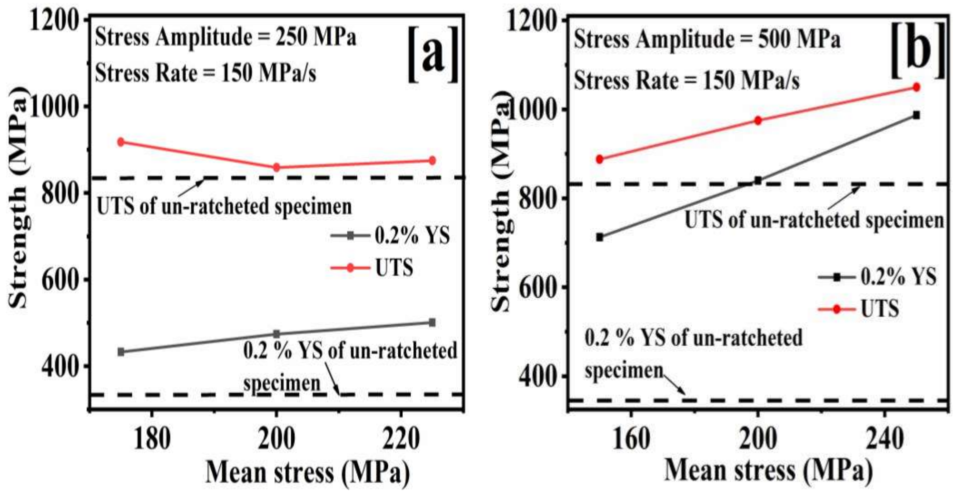

Fig. 6.8 Variation of strength parameters of the Inconel 617 alloy, pre-ratcheted at different mean stresses, at the maximum stress near: (a) yield strength and (b) ultimate tensile strength.

(b) Tensile properties of the Inconel 617 alloy pre-ratcheted at various stress amplitudes

Tensile properties of the alloy pre-ratcheted in two different regions, at different stress amplitudes of 225 to 500 MPa, at a constant mean stress of 200 MPa and stress rate of 150 MPa/s, are summarized in Tables 6.11 and 6.12.

Behaviour similar to that of the mean stress effect was observed. With rise in stress amplitude, the strength parameter S_{YS} increased upto 200% as observed in Fig. 6.9 (a and b) whereas, ductility and degree of work hardening decreased after pre-ratcheting.

Table 6.11 Tensile data of the Inconel 617 alloy pre-ratcheted at different stress amplitudes, at maximum stress near the yield strength (S_{YS}).

Stress amplitude σ_a (MPa)	Strength Parameters			Ductility Parameters			Work hardening Parameters		Degree of work hardening
	Yield strength (MPa)	% Increase in Yield strength	Ultimate tensile strength (MPa)	Uniform Plastic elongation (%)	% Decrease in Uniform Plastic elongation	Total elongation (%)	Strength coefficient (MPa)	Strain hardening exponent	Ultimate tensile strength / Yield strength
Un-ratcheted	347	-	835	54.5	-	66.6	1579	0.36	2.41
225	470	35.4	844	52.0	4.6	62.0	1542	0.32	1.79
250	474	36.6	859	51.0	6.4	61.0	1788	0.41	1.81
275	490	41.2	850	48.5	11.0	59.6	1725	0.38	1.73

Table 6.12 Tensile data of the Inconel 617 alloy pre-ratcheted at different stress amplitudes, at maximum stress near the ultimate tensile strength (S_{UTS}).

Stress amplitude σ_a (MPa)	Strength Parameters			Ductility Parameters			Work hardening Parameters		Degree of work hardening
	Yield strength (MPa)	% Increase in Yield strength	Ultimate tensile strength (MPa)	Uniform Plastic elongation (%)	% Decrease in Uniform Plastic elongation	Total elongation (%)	Strength coefficient (MPa)	Strain hardening exponent	Ultimate tensile strength / Yield strength
Un-ratcheted	347	-	835	54.5	-	66.6	1579	0.36	2.41
450	750	116.1	940	33.2	39.0	48.7	1652	0.25	1.79
500	841	142.3	975	29.5	45.9	46.8	1557	0.18	1.81
550	1039	199.4	1067	10.2	81.3	19.5	1297	0.05	1.73

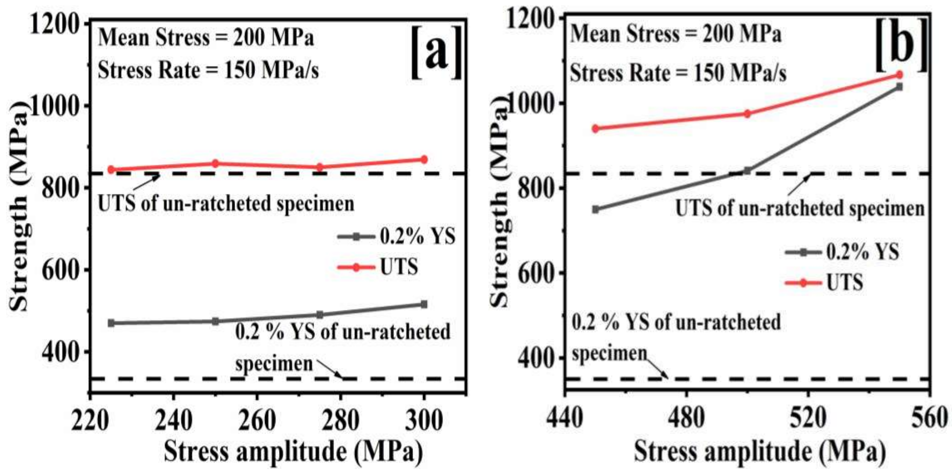

Fig. 6.9 Variation of strength parameters of Inconel 617 alloy pre-ratcheted at different stress amplitudes, at the maximum stress near: (a) yield strength and (b) ultimate tensile strength**.**

(c) Tensile properties of the Inconel 617 alloy pre-ratcheted at various stress rates

The tensile properties of the specimens subjected to asymmetrical loading for 200 cycles at different stress rates of 50, 150 and 450 MPa/s at constant mean stress of 200 MPa and stress amplitude of 450 MPa near the yield strength and at constant mean stress of 200 MPa and stress amplitude of 500 MPa near the ultimate tensile strength are shown in Tables 6.13 and 6.14.

It was observed that on varying stress rate, S_{YS} and S_{UTS} increased with respect to un-ratcheted sample but with rise in stress rate, the S_{YS} decreased and no trend was observed for S_{UTS} as shown in Fig.6.10 (a and b). Contrary to it, the uniform elongation and degree of work hardening increased with increase in stress rate

Table 6.13 Tensile data of the Inconel 617 alloy pre-ratcheted at different stress rates, at maximum stress near the yield strength (S_{YS}).

Stress rate $\dot{\sigma}$ (MPa/s)	Strength parameters			Ductility parameters			Work hardening parameters		Degree of work hardening
	Yield strength (MPa)	% Increase in Yield strength	Ultimate tensile strength (MPa)	Uniform Plastic elongation (%)	% Decrease in Uniform Plastic elongation	Total elongation (%)	Strength coefficient (MPa)	Strain hardening exponent	Ultimate tensile strength / Yield strength
Un-ratcheted	347		835	54.5		66.6	1579	0.36	2.41
50	482	38.9	843	43.5	20.1	54.0	1697	0.38	1.75
150	474	36.6	859	51.0	6.4	61.0	1788	0.41	1.81
450	470	35.4	877	52.6	3.5	62.0	1782	0.39	1.87

Table 6.14 Tensile data of the Inconel 617 alloy pre-ratcheted at different stress rates, at maximum stress near the ultimate tensile strength (S_{UTS}).

Stress rate $\dot{\sigma}$ (MPa/s)	Strength parameters			Ductility parameters			Work hardening parameters		Degree of work hardening
	Yield strength (MPa)	% Decrease in Yield strength	Ultimate tensile strength (MPa)	Uniform Plastic elongation (%)	% Decrease in Uniform Plastic elongation	Total elongation (%)	Strength coefficient (MPa)	Strain hardening exponent	Ultimate tensile strength / Yield strength
Un-ratcheted	347		835	54.5		66.6	1579	0.36	2.41
50	903	160.2	978	21.6	60.4	33.8	1422	0.12	1.08
150	841	142.3	975	29.5	45.9	46.8	1557	0.18	1.15
450	750	116.1	941	37.0	32.1	48.7	1652	0.25	1.25

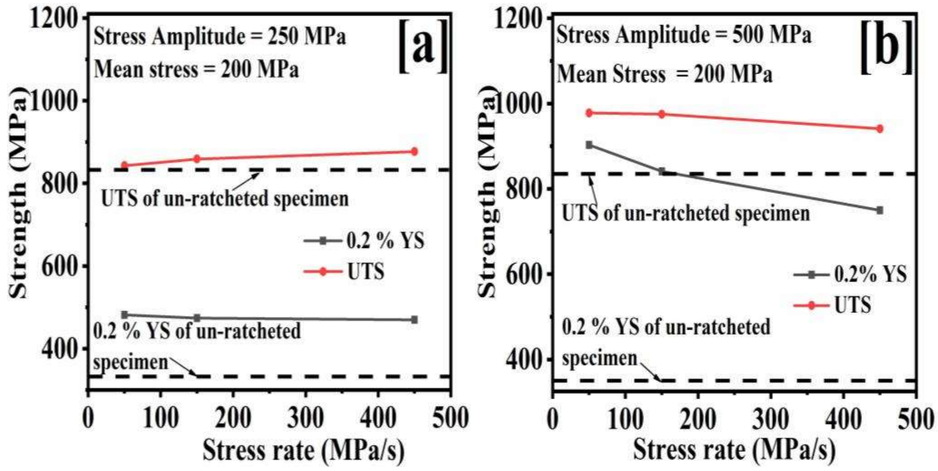

Fig. 6.10 Variation of strength parameters of Inconel 617 alloy pre-ratcheted at different stress rates, at the maximum stress near: (a) yield strength and (b) ultimate tensile strength**.**

6.3.4 Fracture behaviour of Inconel 617 alloy

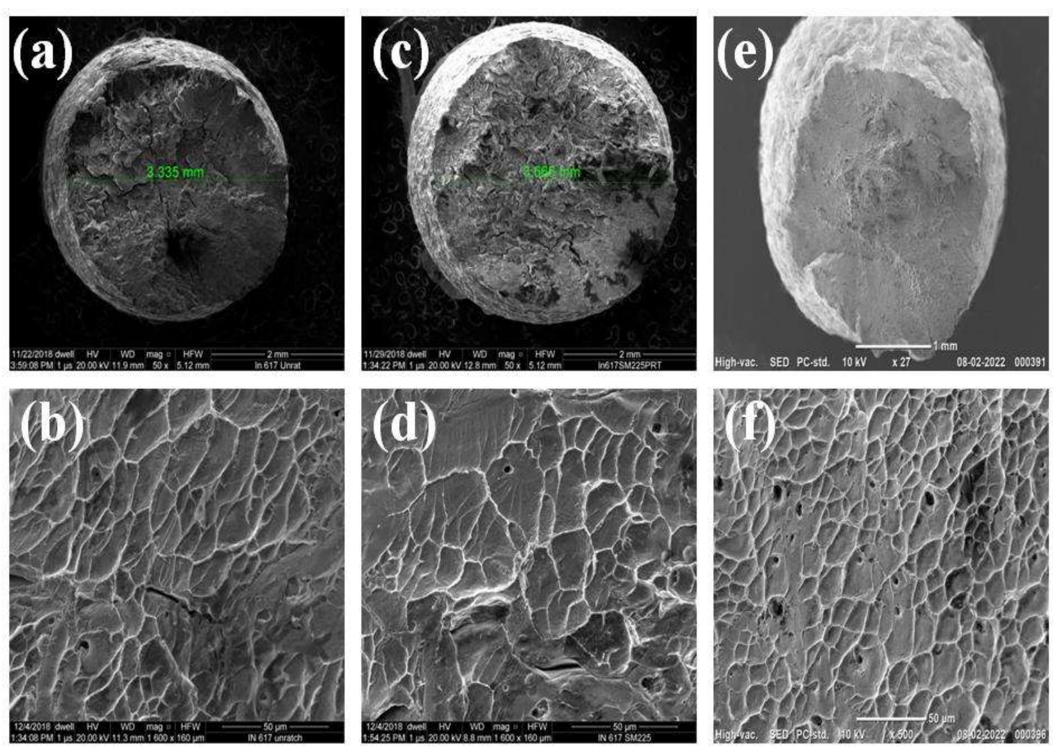

Fig. 6.11 Fracture behaviour of Inconel 617 alloy: (a and b) un-ratcheted specimen and (c and d) ratcheted specimen at maximum stress near yield strength and (e and f) ratcheted specimen at maximum stress near ultimate tensile strength.

The fracture is typical ductile fracture with dimples. Fig. 6.11(a and b) show fractographs of the un-ratcheted specimen and Fig. 6.11(c, d, e and f) show fracture behaviour of the specimens pre-ratcheted at maximum stress near the yield strength and ultimate tensile strength. Fig. 6.11(a, c and e) show lower magnification fractographs and Fig. 6.11(b, d and f) show higher magnification fractographs exhibiting dimples.

6.4. Discussion

6.4 .1 Tensile behaviour of the modified 9 Cr-1Mo steel

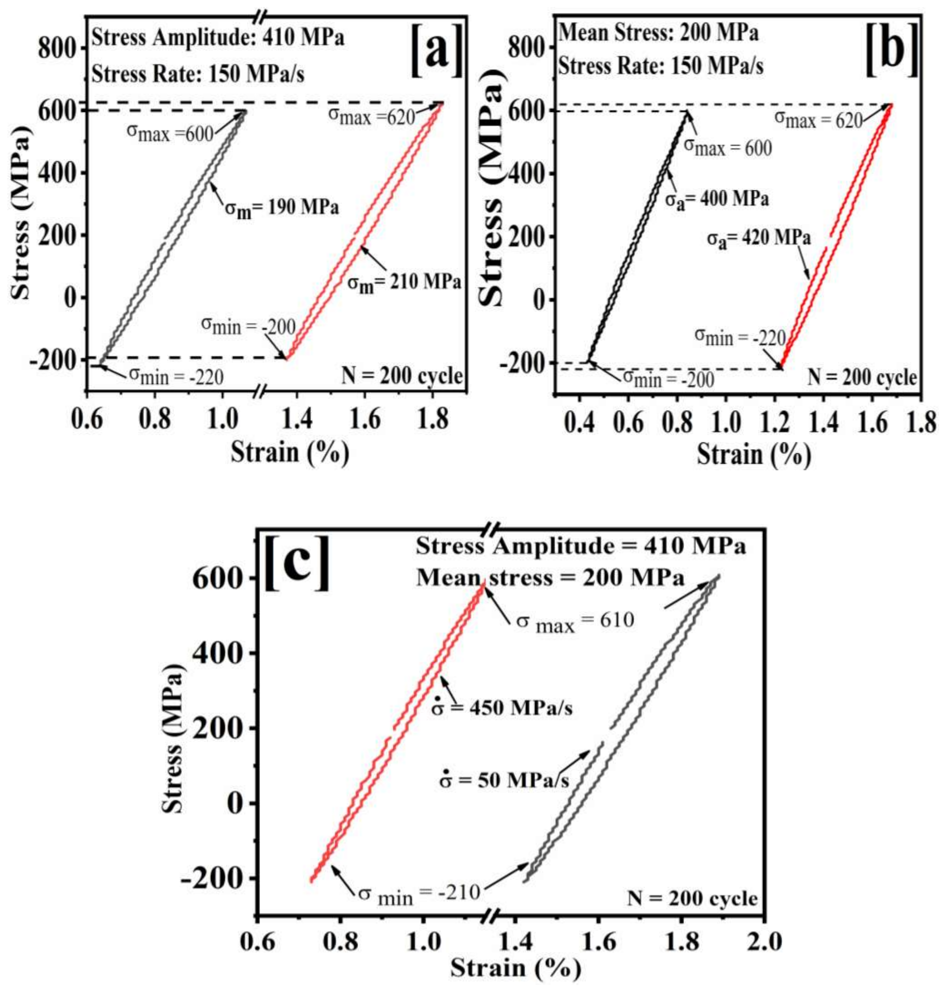

Fig. 6.12 Effect of different variables on hysteresis loops of modified 9Cr-1Mo steel: (a) mean stress (b) stress amplitude and (c) stress rate.

For understanding the ratcheting behaviour of the modified 9Cr-1Mo steel at various combinations of mean stress, stress amplitude and stress rate, hysteresis loops generated during each cycle were recorded. The 200th cycle loops for all the variations were analysed and are depicted in Fig. 6.12(a, b and c). In both the cases, varying mean stress at constant stress amplitude and varying stress amplitude at constant mean stress, the level of maximum stress increased. This induced higher extent of plastic deformation; as a result there was accumulation of larger plastic strain, which caused cyclic hardening of the material under both these parameters (Fig. 6.12a and b). On the other hand, with increase in the stress rate the level of maximum stress remained constant and the loops shifted towards negative strain direction (Fig. 6.12c).The plastic strain accumulation was decreased and the steel did not exhibit cyclic hardening with increase in the stress rate.

Improvement in the yield strength and the reduction in ductility were observed with increase in the mean stress and stress amplitude whereas there was decrease in the yield strength with increase in the stress rate. The reason behind the improvement in yield strength with rise in the mean stress and stress amplitude (Fig. 6.12a and b) is basically due to larger cyclic hardening of the material resulting from increase in the accumulation of plastic strain. The loop energy at 200th cycle is plotted with respect to the yield strength for the various parameters as shown in Fig. 6.13. Area inside a hysteresis loop for that particular cycle is referred as loop energy during ratcheting fatigue. The improvement in yield strength can be well explained on the basis of the loop energy.

Fig. 6.13(a) shows increase in the yield strength with increase in the loop energy, of modified 9Cr-1Mo steel at various mean stresses and stress amplitudes. With increase in the mean stress, hysteresis loop energy increased due to larger accumulation of plastic strain and higher cyclic hardening of the material as a consequence of ratcheting, which resulted in higher yield strength. Fig. 6.13(b) shows that rise in the stress amplitude caused increase in the hysteresis loop energy and consequently the yield strength was increased. During cyclic loading, increase in the stress amplitude means increase in the stress range which simultaneously increases the plastic strain range. Higher plastic strain accumulation results in higher cyclic hardening of the material, as a result the yield strength increases [Dutta et al., (2013)].

On the contrary, reduction in the yield strength was observed with increase in the stress rate (Fig. 6.10c) due to a decrease in the plastic strain accumulation, as seen in Fig. 6.7(e and f). It can be seen from Fig. 6.12(c) that with increase in the stress rate, the hysteresis loop shifted towards lower strain and there was lesser accumulation of the plastic strain. As a consequence, the material softened and the yield strength decreased, similar to that observed earlier in Zircaloy-2 [Rajpurohit et al., (2018)].

Variation in stress rate means increase in it from 50 to 450 MPa/s. As shown in Fig. 6.12c, with increase in stress rate, the cyclic strain hardening in the 200th cycle increased, as is evident with smaller width of the hysteresis loop as compared to that at the lower stress rate of 50 MPa/s. However, the overall accumulated tensile strain in the specimen subjected to 200 cycles, at the highest stress rate of 450 MPa/s was lower than that tested at the low stress rate of 50 MPa/s; therefore, the tensile yield stress of the specimen subjected to higher stress rate is lower than that subjected to lower stress rate.

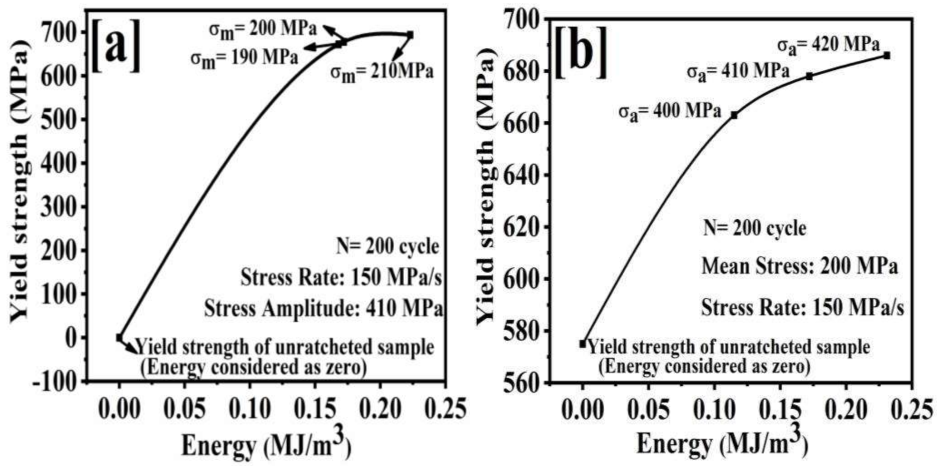

Fig. 6.13 Yield strength vs. hysteresis loop energy of modified 9Cr-1Mo steel at: (a) different mean stresses and (b) different stress amplitudes.

The experimental results were correlated also with the internal microstructural modifications, revealed by TEM. Fig. 6.14(a and b) show bright field micrographs of the un-ratcheted specimen, tested in tensile loading. Segregation of precipitates along the grain boundaries as shown by arrows in Fig. 6.14(a), few dislocations (Fig. 6.14b) and no pile- ups of dislocations can be observed,

At the highest mean stress of 210 MPa, the precipitates are seen to be decorated along the sub grain boundaries as shown by arrows in Fig. 6.14(c), they pin the sub boundaries and thus impart strengthening to material. The diffraction pattern (Fig. 6.14 d) is taken from the same bright field shown in Fig. 6.14(c); it confirms that the spots are from the BCC matrix and from the $M_{23}C_6$ precipitates. In Fig. 6.14(c) an inset of dark field is shown, from the region nearby to that from where the bright field shown in Fig. 6.14(c) was taken. It shows fine spots at the right bottom corner and confirms the presence of particles. In comparison to the un-ratcheted specimen, there is heavy piling up of dislocations and the number density of dislocation has also increased as depicted in Fig. 6.14(e). In the case of stress amplitude, at the highest value of 420 MPa it was observed that solute atmospheres surround the dislocations and interact, it is an additional feature that is depicted in Fig. 6.14(f) leading to an enhancement in strength of the material.

As opposed to the above positive effects of increase in the tensile mean stress and stress amplitude on strengthening, there was a decrease in strength with increase in the stress rate. In addition, shearing of precipitates ($M_{23}C_6$) took place at the highest stress rate, as shown in Fig. 6.14(g) (a clear magnified view is given in Fig. 6.14(h)). The precipitate-matrix interfaces are semi-coherent. This effect of mean stress and stress amplitude is attributed to the observed less effective cyclic hardening.

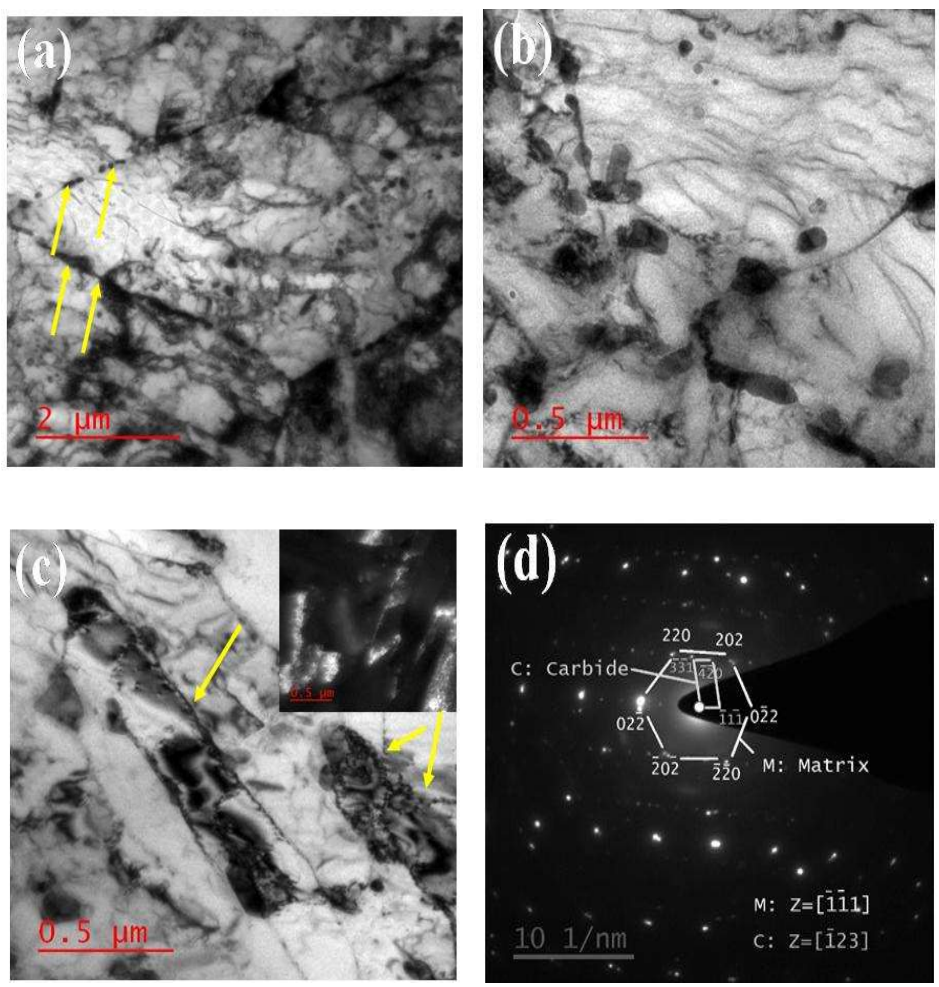

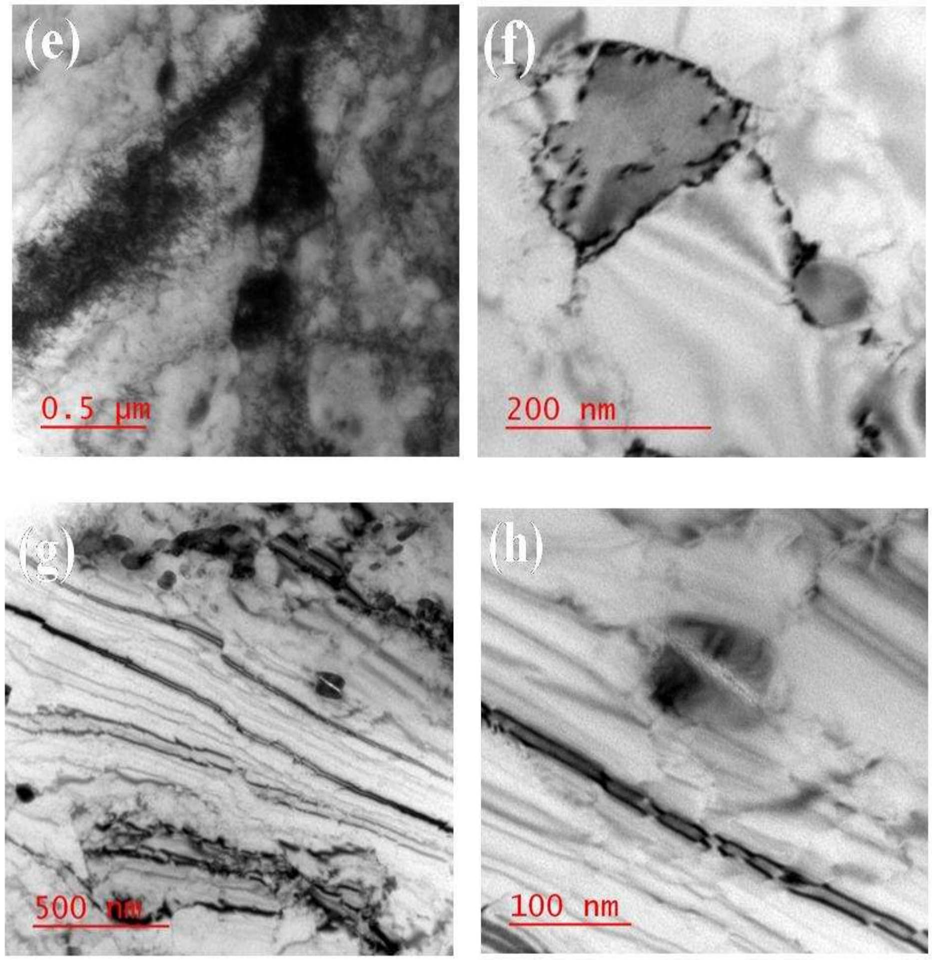

Fig. 6.14 (a and b) TEM Bright field micrographs of modified 9Cr-1Mo steel for un-ratcheted specimen (c) Bright field micrograph for mean stress of 210 MPa, stress amplitude of 410 MPa, stress rate of 150 MPa/s indicating pinning of boundaries by precipitate with an inset showing dark field (d) Diffraction pattern confirming BCC matrix and FCC precipitate ($Cr_{23}C_6$) for mean stress of 210 MPa, stress amplitude of 410 MPa, stress rate of 150 MPa/s (e) Bright field micrograph for mean stress of 210 MPa, stress amplitude of 410 MPa, stress rate of 150 MPa/s showing heavy dislocation pile up (f) Bright field micrographs for stress amplitude of 420 MPa, mean stress of 200 MPa, stress rate of 150 MPa/s depicting interaction of dislocation with solute atmosphere (g and h) Bright field micrographs for stress rate of 450 MPa/s, mean stress of 200 MPa, stress amplitude of 410 MPa showing shearing of the precipitate ($M_{23}C_6$).

6.4.2 Tensile behaviour of the Inconel 617 alloy

A similar behaviour was observed in Inconel 617 alloy as in case of modified 9Cr-1Mo steel. For the Inconel 617 alloy also the 200th cycle loops corresponding to all the variations were analysed and are depicted in Fig. 6.15(a, b and c). In both the cases, varying mean stress at constant stress amplitude and varying stress amplitude at constant mean stress, the level of maximum stress increased. This induced higher extent of plastic deformation; as a result there was accumulation of larger plastic strain, which caused cyclic hardening of the material under both these parameters (Fig. 6.15a and b). On the other hand, with increase in the stress rate the level of maximum stress remained constant and the loops shifted towards negative strain direction (Fig. 6.15c). Plastic strain accumulation was decreased and the material did not exhibit cyclic hardening with increase in the stress rate.

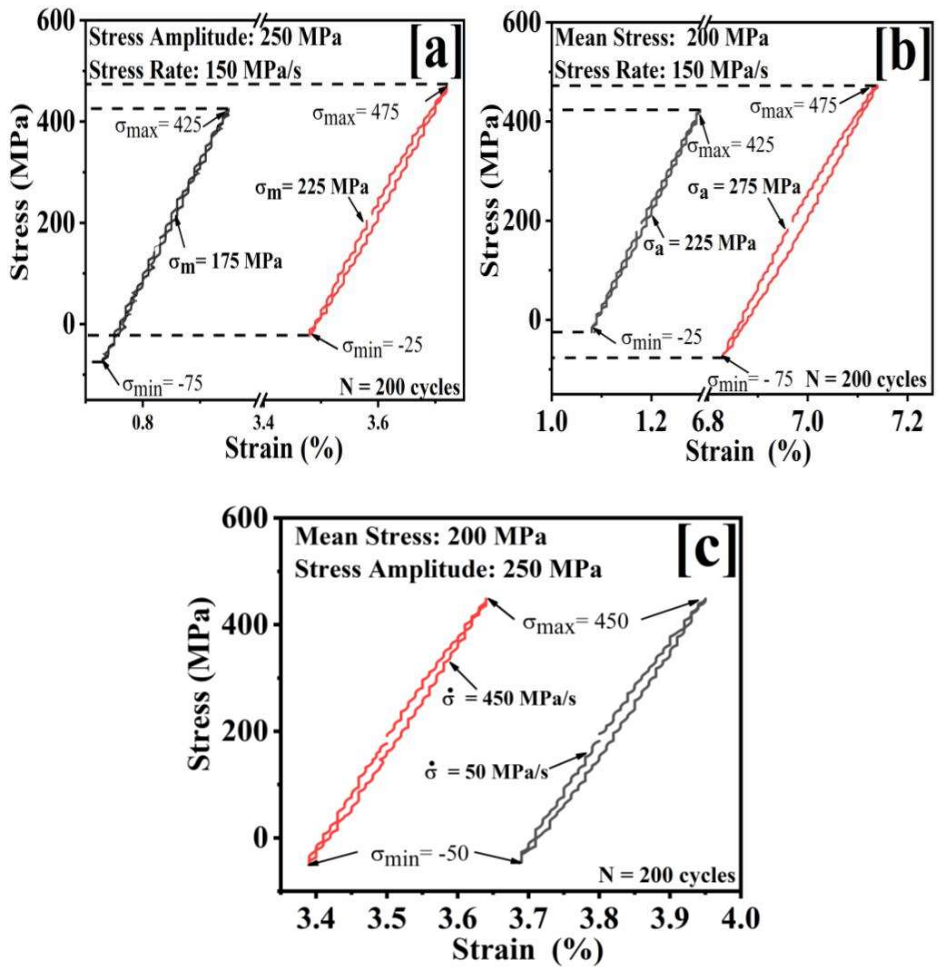

Fig. 6.15 Effect of different variables on hysteresis loops of Inconel 617 alloy at: (a) different mean stress (b) different stress amplitudes and (c) different stress rates.

In case of Inconel 617 alloy, the microstructural characterization of the un-ratcheted specimen depicted deformation with the aid of slip (Fig. 6.16a). The dislocations are randomly distributed (Fig. 6.16b). The slip bands and randomly arranged dislocations are found throughout the microstructure and are visible depending upon the orientation of grains.

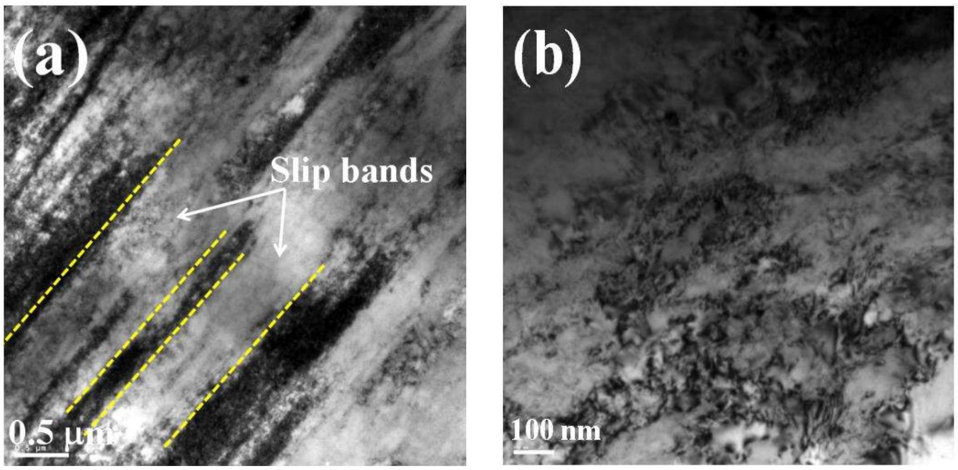

Fig. 6.16 TEM Bright field micrographs for un-ratcheted specimen of Inconel 617 alloy showing: (a) slip bands and (b) dislocation sub-structure.

When the specimens were subjected to cyclic loading and later got fractured due to tensile loading the deformation depicted twinning (Fig. 6.17a) across (200) planes. This twinning behaviour can be observed in bright field and its corresponding diffraction pattern shown in Fig. 6.17 (a and b), respectively. Both the twinned regions are mutually rotated at 7^{o}. Similar twinned regions can also be observed in Fig. 6.17(c). Comparison on the basis of number of dislocations between Fig. 6.16(b) and Fig. 6.17(c) confirms pile up of dislocations along twin planes signifying increase in the strength parameters. The ratcheted sample (Fig. 6.16b) shows higher dislocation concentration as compared to the un-ratcheted one (Fig. 6.17c).

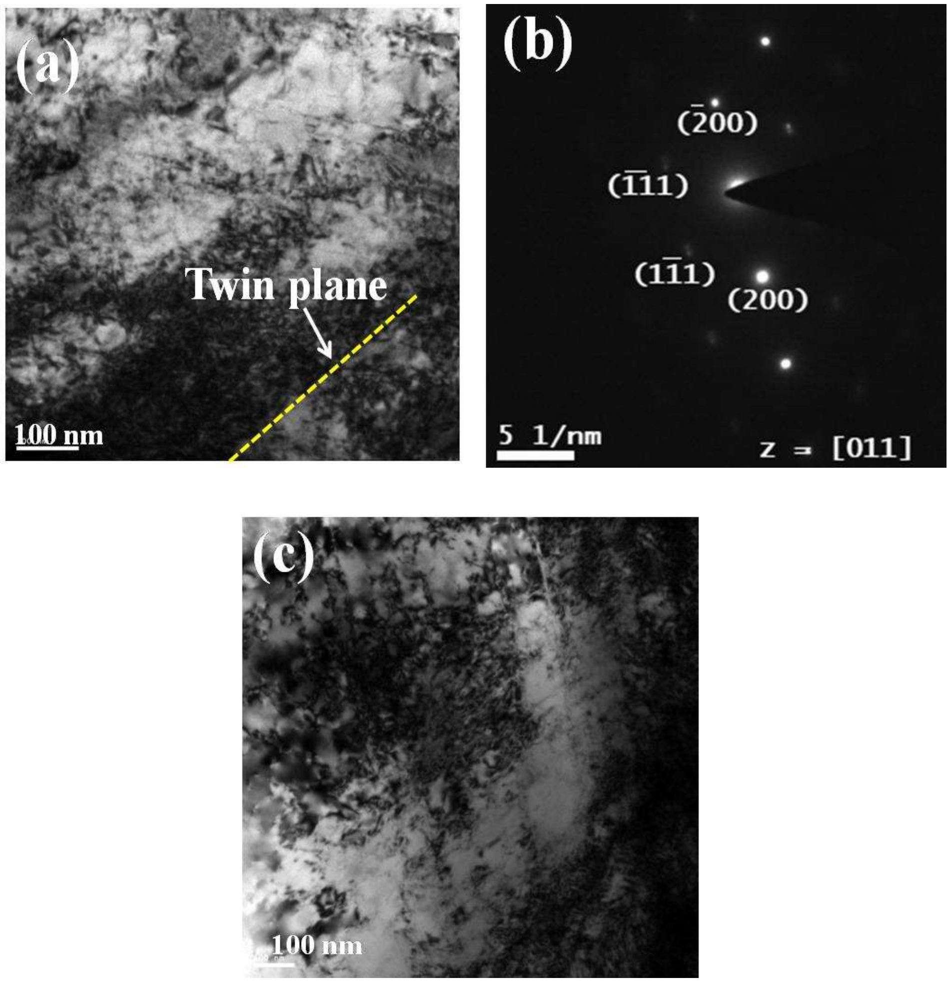

Fig. 6.17 TEM Bright field micrographs of Inconel 617 alloy ratcheted at the maximum stress near the yield strength at stress amplitude of 275 MPa and at constant mean stress of 200 MPa and stress rate of 150 MPa/s showing: (a) twinning (b) corresponding diffraction pattern showing twin plane and (c) dislocation sub-structure.

6.5 Summary

The important inferences that can be drawn from the effect of pre-ratcheting behaviour of the two alloys on tensile properties are listed below:

1. The accumulated ratcheting strain increased with increase in the mean stress and stress amplitude and decreased with increase in the stress rate for the two alloys.

2. Tensile data of the pre-ratcheted specimens showed increase in the strength parameters and decrease in the ductility parameters for modified 9Cr-1Mo steel and Inconel 617 alloy.
3. For modified 9Cr-1Mo steel, the values of strength parameters for the ratcheted specimens were higher than those of the un-ratcheted one. The increase in the yield strength was about 21% and in the ultimate tensile strength was about 13%, with respect to the un-ratcheted sample. On the other hand, the ductility of the ratcheted specimen decreased 12% with respect to that of un-ratcheted specimen.
4. Like that in the modified 9Cr -1Mo steel, for Inconel 617 alloy, the values of strength parameters increased in comparison to the un-ratcheted one. There was marked increase in yield strength of the Inconel 617 alloy by about 200% and the ultimate tensile strength by 28%. There was decrease in ductility of about 69% as compared to that of the un-ratcheted specimen.
5. Fractographs of the ratcheted specimens of modified 9Cr-1Mo steel showed both dimples and striations like features whereas the fracture surface of the un-ratcheted specimen exhibited rosette fracture. In case of Inconel 617 alloy, both the ratcheted and un-ratcheted specimen exhibited purely tensile fracture showing dimples.
6. The reason for the difference in fracture surfaces of the 9Cr-1Mo steel and Inconel 617 alloy is due to difference in their crystal structure, the types of second phase particles and their distribution.
7. For the modified 9Cr-1Mo steel, the TEM analysis revealed that with increase in the mean stress, there was an increase in number of dislocations, the particles pinned the boundaries and imparted strength to material. In the case of rise in stress amplitude, solute atmospheres surrounded the dislocations and interaction

between them enhanced the strength. On the other hand, increase in stress rate resulted in shearing of the precipitates due to which there was less effective cyclic hardening of the material and the strength was decreased.

8. Deformation behaviour of Inconel 617 alloy revealed formation of slip bands for un-ratcheted specimen whereas twinning was observed for ratcheted specimen. There was increase in dislocation concentration for ratcheted specimen.